

New Low-Dissipation Central-Upwind Schemes. Part II

Shaoshuai Chu*, Alexander Kurganov† and Ruixiao Xin‡

Abstract

The low-dissipation central-upwind (LDCU) schemes have been recently introduced in [A. KURGANOV AND R. XIN, J. SCI. COMPUT., 96 (2023), PAPER No. 56] as a modification of the central-upwind (CU) schemes from [A. KURGANOV AND C. T. LIN, COMMUN. COMPUT. PHYS., 2 (2007), PP. 141-163]. The LDCU schemes achieve much higher resolution of contact waves and many (two-dimensional) structures resulting from complicated wave interaction. However, the LDCU schemes sometimes produce more oscillatory results compared with the CU schemes, especially near the computational domain boundaries.

In this paper, we propose a very simple—yet systematic—modification of the LDCU schemes, which completely eliminates the aforementioned oscillations almost without affecting the quality of the computed solution.

Key words: Hyperbolic systems of conservation laws, low-dissipation central-upwind schemes, Euler equations of gas dynamics.

AMS subject classification: 76M12, 65M08, 76N15, 35L65, 35L67.

1 Introduction

We consider hyperbolic systems of conservation laws, which in the one-dimensional (1-D) case read as

$$\mathbf{U}_t + \mathbf{F}(\mathbf{U})_x = \mathbf{0}, \quad (1.1)$$

and in the two-dimensional (2-D) case read as

$$\mathbf{U}_t + \mathbf{F}(\mathbf{U})_x + \mathbf{G}(\mathbf{U})_y = \mathbf{0}, \quad (1.2)$$

where x and y are spatial variables, t is the time, $\mathbf{U} \in \mathbb{R}^d$ is a vector of unknowns, and \mathbf{F} and \mathbf{G} are the x - and y -directional fluxes, respectively.

We focus on finite-volume central-upwind (CU) schemes, which were introduced in [4, 6, 7] as a “black-box” solver for general hyperbolic systems (1.1) and (1.2). Even though the CU

*Department of Mathematics and Shenzhen International Center for Mathematics, Southern University of Science and Technology, Shenzhen, 518055, China; chuss@mail.sustech.edu.cn

†Department of Mathematics, Shenzhen International Center for Mathematics, and Guangdong Provincial Key Laboratory of Computational Science and Material Design, Southern University of Science and Technology, Shenzhen, 518055, China; alexander@sustech.edu.cn

‡Department of Mathematics, Southern University of Science and Technology, Shenzhen, 518055, China; 12331009@mail.sustech.edu.cn

schemes are quite accurate, efficient, and robust for a wide variety of hyperbolic systems, higher resolution of the numerical solutions can be achieved by further reducing numerical dissipation present in the CU schemes; see, e.g., [1, 5, 8]. The low-dissipation CU (LDCU) schemes have been recently proposed in [8] as a modification of the CU scheme from [5]. The LDCU schemes achieve much higher resolution of contact waves and many (two-dimensional) structures resulting from complicated wave interaction. However, the LDCU schemes sometimes produce more oscillatory results compared with the CU schemes, especially near the computational domain boundaries.

In order to suppress these spurious oscillations, we modify both 1-D and 2-D LDCU schemes. The proposed modifications are very simple, yet systematic as they are based on a more accurate projection of the evolved solution onto the original (uniform) mesh. The new LDCU schemes are developed for the 1-D and 2-D Euler equations of gas dynamics and tested on several numerical examples. The obtained numerical results demonstrate that the new schemes contain almost the same small amount of numerical dissipation as the LDCU schemes from [8] but produce substantially “cleaner”, non-oscillatory computed solutions.

2 New LDCU Schemes

We follow the derivation of the LDCU scheme in [8] and use precisely the same notation as in [8].

We cover the computational domain with the finite volume cells $C_j = [x_{j-\frac{1}{2}}, x_{j+\frac{1}{2}}]$, $j = 1, \dots, N$, which are assumed to be uniform, that is, $x_{j+\frac{1}{2}} - x_{j-\frac{1}{2}} \equiv \Delta x$. We then assume that the solution, realized in terms of its cell averages \bar{U}_j^n , is available at a certain time level $t = t^n$ and reconstruct a second-order piecewise linear interpolant $\sum_j [\bar{U}_j^n + (U_x)_j^n (x - x_j)] \mathcal{X}_{C_j}$, where \mathcal{X} denotes the characteristic function of the corresponding intervals and $(U_x)_j^n$ are the slopes obtained using a nonlinear limiter. In the numerical experiments reported in §3, we have used a generalized minmod limiter with the minmod parameter $\theta = 1.3$; see, e.g., [9, 11, 15, 16].

We then evaluate the local speeds of propagation $a_{j+\frac{1}{2}}^\pm$, introduce the corresponding points $x_{j+\frac{1}{2},\ell}^n := x_{j+\frac{1}{2}} + a_{j+\frac{1}{2}}^- \Delta t^n$ and $x_{j+\frac{1}{2},r}^n := x_{j+\frac{1}{2}} + a_{j+\frac{1}{2}}^+ \Delta t^n$, and integrate the system (1.1) over the space-time control volumes consisting of the “smooth” $[x_{j-\frac{1}{2},r}, x_{j+\frac{1}{2},\ell}] \times [t^n, t^{n+1}]$ and “nonsmooth” $[x_{j+\frac{1}{2},\ell}, x_{j+\frac{1}{2},r}] \times [t^n, t^{n+1}]$ areas, where $t^{n+1} := t^n + \Delta t^n$. This way the solution is evolved in time and upon the completion of the evolution step, we obtain the intermediate cell averages $\bar{U}_{j+\frac{1}{2}}^{\text{int}}$ (see [8, Eq. (2.7)]) and \bar{U}_j^{int} (see [8, Eq. (2.10)]).

Next, the intermediate solution, which is realized in terms of $\{\bar{U}_j^{\text{int}}\}$ and $\{\bar{U}_{j+\frac{1}{2}}^{\text{int}}\}$, is projected onto the original grid. To this end, we need to construct the interpolant

$$\tilde{U}^{\text{int}}(x) = \sum_j \left\{ \tilde{U}_{j+\frac{1}{2}}^{\text{int}}(x) \mathcal{X}_{[x_{j+\frac{1}{2},\ell}, x_{j+\frac{1}{2},r}]} + \bar{U}_j^{\text{int}} \mathcal{X}_{[x_{j-\frac{1}{2},r}, x_{j+\frac{1}{2},\ell}]} \right\}. \quad (2.1)$$

In order to develop the original LDCU scheme in [8], we have used

$$\tilde{U}_{j+\frac{1}{2}}^{\text{int}}(x) = \begin{cases} \bar{U}_{j+\frac{1}{2}}^{\text{int,L}}, & x < x_{j+\frac{1}{2}}, \\ \bar{U}_{j+\frac{1}{2}}^{\text{int,R}}, & x > x_{j+\frac{1}{2}}, \end{cases} \quad (2.2)$$

where $\tilde{U}_{j+\frac{1}{2}}^{\text{int}}(x)$ is discontinuous at $x = x_{j+\frac{1}{2}}$. The values $\bar{U}_{j+\frac{1}{2}}^{\text{int,L}}$ and $\bar{U}_{j+\frac{1}{2}}^{\text{int,R}}$ are determined based

on the conservation requirement

$$a_{j+\frac{1}{2}}^+ \bar{U}_{j+\frac{1}{2}}^{\text{int,R}} - a_{j+\frac{1}{2}}^- \bar{U}_{j+\frac{1}{2}}^{\text{int,L}} = (a_{j+\frac{1}{2}}^+ - a_{j+\frac{1}{2}}^-) \bar{U}_{j+\frac{1}{2}}^{\text{int}}. \quad (2.3)$$

and d additional degrees of freedom, which can be used to design an accurate projection. The way these degrees freedom are utilized depends on the problem at hand. One, however, can introduce an additional degree of freedom, which may be used to further improve the accuracy of the projection step.

2.1 Modification of the Projection Step

We propose to replace (2.2) with

$$\tilde{U}_{j+\frac{1}{2}}^{\text{int}}(x) = \begin{cases} \bar{U}_{j+\frac{1}{2}}^{\text{int,L}}, & x < \tilde{x}_{j+\frac{1}{2}}, \\ \bar{U}_{j+\frac{1}{2}}^{\text{int,R}}, & x > \tilde{x}_{j+\frac{1}{2}}, \end{cases} \quad (2.4)$$

where $\tilde{x}_{j+\frac{1}{2}} = x_{j+\frac{1}{2}} + \tilde{u}_{j+\frac{1}{2}} \Delta t^n$ and $\tilde{u}_{j+\frac{1}{2}} \in (a_{j+\frac{1}{2}}^-, a_{j+\frac{1}{2}}^+)$ represents an additional degree of freedom. The conservation requirements now give

$$(a_{j+\frac{1}{2}}^+ - \tilde{u}_{j+\frac{1}{2}}) \bar{U}_{j+\frac{1}{2}}^{\text{int,R}} + (\tilde{u}_{j+\frac{1}{2}} - a_{j+\frac{1}{2}}^-) \bar{U}_{j+\frac{1}{2}}^{\text{int,L}} = (a_{j+\frac{1}{2}}^+ - a_{j+\frac{1}{2}}^-) \bar{U}_{j+\frac{1}{2}}^{\text{int}}; \quad (2.5)$$

compare with (2.3), which is obtained from (2.5) if $\tilde{u}_{j+\frac{1}{2}} = 0$. The modified projection step is outlined in Figure 2.1; compare it with [8, Fig. 3].

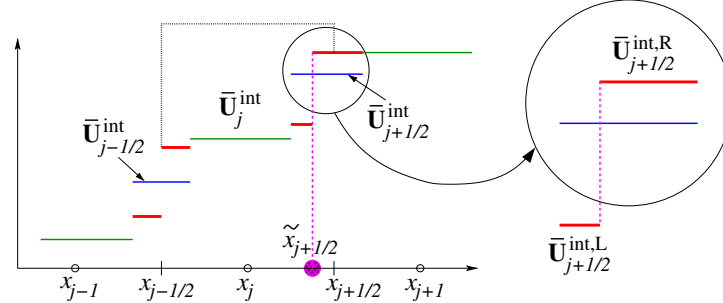


Figure 2.1: The new projection step.

In order to complete the derivation of the new LDCU scheme, we need to consider a particular hyperbolic system. As in [8], we study the Euler equation of gas dynamics.

2.2 New LDCU Scheme for the 1-D Euler Equations of Gas Dynamics

The 1-D Euler equations of gas dynamics reads as (1.1) with $\mathbf{U} = (\rho, \rho u, E)^\top$ and $\mathbf{F}(\mathbf{U}) = (\rho u, \rho u^2 + p, u(E + p))^\top$, where ρ is the density, u is the velocity, p is the pressure, and E is the total energy. The system is closed using the equation of states (EOS), which is in the case of ideal gas is $p = (\gamma - 1)[E - \frac{1}{2}\rho u^2]$, $\gamma = \text{Const}$.

In order to derive the new LDCU scheme for the 1-D Euler equations, we first follow [8, §3.1] to obtain the point values $\rho_{j+\frac{1}{2}}^\pm$, $(\rho u)_{j+\frac{1}{2}}^\pm$, and $E_{j+\frac{1}{2}}^\pm$, evaluate the corresponding point values $u_{j+\frac{1}{2}}^\pm$ and $p_{j+\frac{1}{2}}^\pm$, and estimate the one-sided local speeds of propagation $a_{j+\frac{1}{2}}^\pm$.

We then proceed with the evolution of the subcell averages $\bar{U}_{j+\frac{1}{2}}^{\text{int,L}} = (\bar{\rho}_{j+\frac{1}{2}}^{\text{int,L}}, (\bar{\rho}u)_{j+\frac{1}{2}}^{\text{int,L}}, \bar{E}_{j+\frac{1}{2}}^{\text{int,L}})^\top$ and $\bar{U}_{j+\frac{1}{2}}^{\text{int,R}} = (\bar{\rho}_{j+\frac{1}{2}}^{\text{int,R}}, (\bar{\rho}u)_{j+\frac{1}{2}}^{\text{int,R}}, \bar{E}_{j+\frac{1}{2}}^{\text{int,R}})^\top$ required in (2.4). Similarly to [8, §3], we enforce the continuity of u and p across the cell interfaces by setting

$$u_{j+\frac{1}{2}}^{\text{int,L}} := \frac{(\bar{\rho}u)_{j+\frac{1}{2}}^{\text{int,L}}}{\bar{\rho}_{j+\frac{1}{2}}^{\text{int,L}}} = \frac{(\bar{\rho}u)_{j+\frac{1}{2}}^{\text{int,R}}}{\bar{\rho}_{j+\frac{1}{2}}^{\text{int,R}}} =: u_{j+\frac{1}{2}}^{\text{int,R}}, \quad \bar{E}_{j+\frac{1}{2}}^{\text{int,L}} - \frac{((\bar{\rho}u)_{j+\frac{1}{2}}^{\text{int,L}})^2}{2\bar{\rho}_{j+\frac{1}{2}}^{\text{int,L}}} = \bar{E}_{j+\frac{1}{2}}^{\text{int,R}} - \frac{((\bar{\rho}u)_{j+\frac{1}{2}}^{\text{int,R}})^2}{2\bar{\rho}_{j+\frac{1}{2}}^{\text{int,R}}}. \quad (2.6)$$

Next, (2.6) together with the conservation requirement (2.5) applied to ρ , ρu , and E ,

$$\begin{aligned} (a_{j+\frac{1}{2}}^+ - \tilde{u}_{j+\frac{1}{2}}) \bar{\rho}_{j+\frac{1}{2}}^{\text{int,R}} + (\tilde{u}_{j+\frac{1}{2}} - a_{j+\frac{1}{2}}^-) \bar{\rho}_{j+\frac{1}{2}}^{\text{int,L}} &= (a_{j+\frac{1}{2}}^+ - a_{j+\frac{1}{2}}^-) \bar{\rho}_{j+\frac{1}{2}}^{\text{int}}, \\ (a_{j+\frac{1}{2}}^+ - \tilde{u}_{j+\frac{1}{2}}) (\bar{\rho}u)_{j+\frac{1}{2}}^{\text{int,R}} + (\tilde{u}_{j+\frac{1}{2}} - a_{j+\frac{1}{2}}^-) (\bar{\rho}u)_{j+\frac{1}{2}}^{\text{int,L}} &= (a_{j+\frac{1}{2}}^+ - a_{j+\frac{1}{2}}^-) (\bar{\rho}u)_{j+\frac{1}{2}}^{\text{int}}, \\ (a_{j+\frac{1}{2}}^+ - \tilde{u}_{j+\frac{1}{2}}) \bar{E}_{j+\frac{1}{2}}^{\text{int,R}} + (\tilde{u}_{j+\frac{1}{2}} - a_{j+\frac{1}{2}}^-) \bar{E}_{j+\frac{1}{2}}^{\text{int,L}} &= (a_{j+\frac{1}{2}}^+ - a_{j+\frac{1}{2}}^-) \bar{E}_{j+\frac{1}{2}}^{\text{int}}, \end{aligned} \quad (2.7)$$

yield a system of five algebraic equations (2.6)–(2.7), which we solve for $(\bar{\rho}u)_{j+\frac{1}{2}}^{\text{int,L}}$, $(\bar{\rho}u)_{j+\frac{1}{2}}^{\text{int,R}}$, $\bar{E}_{j+\frac{1}{2}}^{\text{int,L}}$, and $\bar{E}_{j+\frac{1}{2}}^{\text{int,R}}$, and express these quantities in terms of $\bar{\rho}_{j+\frac{1}{2}}^{\text{int,L}}$ and $\bar{\rho}_{j+\frac{1}{2}}^{\text{int,R}}$:

$$\begin{aligned} (\bar{\rho}u)_{j+\frac{1}{2}}^{\text{int,L}} &= \bar{\rho}_{j+\frac{1}{2}}^{\text{int,L}} u_{j+\frac{1}{2}}^{\text{int}}, & (\bar{\rho}u)_{j+\frac{1}{2}}^{\text{int,R}} &= \bar{\rho}_{j+\frac{1}{2}}^{\text{int,R}} u_{j+\frac{1}{2}}^{\text{int}}, \\ \bar{E}_{j+\frac{1}{2}}^{\text{int,L}} &= \bar{E}_{j+\frac{1}{2}}^{\text{int}} + \frac{\bar{\rho}_{j+\frac{1}{2}}^{\text{int,L}} - \rho_{j+\frac{1}{2}}^{\text{int}}}{2} (u_{j+\frac{1}{2}}^{\text{int}})^2, & \bar{E}_{j+\frac{1}{2}}^{\text{int,R}} &= \bar{E}_{j+\frac{1}{2}}^{\text{int}} + \frac{\bar{\rho}_{j+\frac{1}{2}}^{\text{int,R}} - \rho_{j+\frac{1}{2}}^{\text{int}}}{2} (u_{j+\frac{1}{2}}^{\text{int}})^2, \end{aligned} \quad (2.8)$$

where $u_{j+\frac{1}{2}}^{\text{int}} := (\bar{\rho}u)_{j+\frac{1}{2}}^{\text{int}} / \bar{\rho}_{j+\frac{1}{2}}^{\text{int}}$.

Note that the first two equations in (2.8) give $u_{j+\frac{1}{2}}^{\text{int,L}} = u_{j+\frac{1}{2}}^{\text{int}} = u_{j+\frac{1}{2}}^{\text{int,R}}$, which suggests that in this piecewise constant solution approximation, the velocity is constant in $[x_{j+\frac{1}{2},\ell}, x_{j+\frac{1}{2},r}]$. We therefore use the same velocity value and set $\tilde{u}_{j+\frac{1}{2}} = u_{j+\frac{1}{2}}^{\text{int}}$.

Finally, we follow the steps in [8, §3], where we make the difference $\bar{\rho}_{j+\frac{1}{2}}^{\text{int,R}} - \bar{\rho}_{j+\frac{1}{2}}^{\text{int,L}}$ as large as possible without creating any new local extrema. To this end, we denote by

$$S_{j+\frac{1}{2}}^- := (u_{j+\frac{1}{2}}^{\text{int}} - a_{j+\frac{1}{2}}^-) (\bar{\rho}_{j+\frac{1}{2}}^{\text{int}} - \rho_{j+\frac{1}{2},\ell}^{\text{int}}) \quad \text{and} \quad S_{j+\frac{1}{2}}^+ := (a_{j+\frac{1}{2}}^+ - u_{j+\frac{1}{2}}^{\text{int}}) (\rho_{j+\frac{1}{2},r}^{\text{int}} - \bar{\rho}_{j+\frac{1}{2}}^{\text{int}}),$$

where the point values $\rho_{j+\frac{1}{2},\ell}^{\text{int}}$ and $\rho_{j+\frac{1}{2},r}^{\text{int}}$ were introduced in [8, Eq. (2.14)], and then determine $\bar{\rho}_{j+\frac{1}{2}}^{\text{int,L}}$ and $\bar{\rho}_{j+\frac{1}{2}}^{\text{int,R}}$ by

$$\begin{aligned} \bar{\rho}_{j+\frac{1}{2}}^{\text{int,L}} &= \bar{\rho}_{j+\frac{1}{2}}^{\text{int}} + \frac{\delta_{j+\frac{1}{2}}}{a_{j+\frac{1}{2}}^- - u_{j+\frac{1}{2}}^{\text{int}}}, \\ \bar{\rho}_{j+\frac{1}{2}}^{\text{int,R}} &= \bar{\rho}_{j+\frac{1}{2}}^{\text{int}} + \frac{\delta_{j+\frac{1}{2}}}{a_{j+\frac{1}{2}}^+ - u_{j+\frac{1}{2}}^{\text{int}}}, \end{aligned} \quad \delta_{j+\frac{1}{2}} := \min\text{mod}(S_{j+\frac{1}{2}}^-, S_{j+\frac{1}{2}}^+); \quad (2.9)$$

compare these formulae with [8, Eq. (3.14)]. Here, $\min\text{mod}(a, b) := \frac{1}{2}(\text{sgn}(a) + \text{sgn}(b)) \min(|a|, |b|)$.

We then substitute (2.9) into (2.8) and obtain

$$\begin{aligned} (\overline{\rho u})_{j+\frac{1}{2}}^{\text{int,L}} &= (\overline{\rho u})_{j+\frac{1}{2}}^{\text{int}} + \frac{\delta_{j+\frac{1}{2}}}{a_{j+\frac{1}{2}}^+ - u_{j+\frac{1}{2}}^{\text{int}}} u_{j+\frac{1}{2}}^{\text{int}}, & (\overline{\rho u})_{j+\frac{1}{2}}^{\text{int,R}} &= (\overline{\rho u})_{j+\frac{1}{2}}^{\text{int}} + \frac{\delta_{j+\frac{1}{2}}}{a_{j+\frac{1}{2}}^+ - u_{j+\frac{1}{2}}^{\text{int}}} u_{j+\frac{1}{2}}^{\text{int}}, \\ \overline{E}_{j+\frac{1}{2}}^{\text{int,L}} &= \overline{E}_{j+\frac{1}{2}}^{\text{int}} + \frac{\delta_{j+\frac{1}{2}}}{2(a_{j+\frac{1}{2}}^+ - u_{j+\frac{1}{2}}^{\text{int}})} (u_{j+\frac{1}{2}}^{\text{int}})^2, & \overline{E}_{j+\frac{1}{2}}^{\text{int,R}} &= \overline{E}_{j+\frac{1}{2}}^{\text{int}} + \frac{\delta_{j+\frac{1}{2}}}{2(a_{j+\frac{1}{2}}^+ - u_{j+\frac{1}{2}}^{\text{int}})} (u_{j+\frac{1}{2}}^{\text{int}})^2. \end{aligned} \quad (2.10)$$

2.2.1 Fully Discrete Scheme

We now derive a new fully discrete LDCU scheme based on the new projection step. To this end, we integrate the piecewise constant interpolant (2.1), (2.4) over the cell C_j and obtain

$$\begin{aligned} \overline{U}_j^{n+1} &= \overline{U}_j^{\text{int}} + \frac{\Delta t^n}{\Delta x} \left[a_{j-\frac{1}{2}}^+ (\overline{U}_{j-\frac{1}{2}}^{\text{int,R}} - \overline{U}_j^{\text{int}}) - a_{j+\frac{1}{2}}^- (\overline{U}_{j+\frac{1}{2}}^{\text{int,L}} - \overline{U}_j^{\text{int}}) \right. \\ &\quad \left. + \max(u_{j-\frac{1}{2}}^{\text{int}}, 0) (\overline{U}_{j-\frac{1}{2}}^{\text{int,L}} - \overline{U}_{j-\frac{1}{2}}^{\text{int,R}}) - \max(u_{j+\frac{1}{2}}^{\text{int}}, 0) (\overline{U}_{j+\frac{1}{2}}^{\text{int,L}} - \overline{U}_{j+\frac{1}{2}}^{\text{int,R}}) \right] \\ &\stackrel{(2.9),(2.10)}{=} \overline{U}_j^{\text{int}} + \frac{\Delta t^n}{\Delta x} \left[a_{j-\frac{1}{2}}^+ (\overline{U}_{j-\frac{1}{2}}^{\text{int}} - \overline{U}_j^{\text{int}}) - a_{j+\frac{1}{2}}^- (\overline{U}_{j+\frac{1}{2}}^{\text{int}} - \overline{U}_j^{\text{int}}) + \alpha_{j-\frac{1}{2}}^{\text{int}} \delta_{j-\frac{1}{2}} - \alpha_{j+\frac{1}{2}}^{\text{int}} \delta_{j+\frac{1}{2}} \right], \end{aligned} \quad (2.11)$$

where

$$\alpha_{j+\frac{1}{2}}^{\text{int}} = \begin{cases} \frac{a_{j+\frac{1}{2}}^+}{a_{j+\frac{1}{2}}^+ - u_{j+\frac{1}{2}}^{\text{int}}} & \text{if } u_{j+\frac{1}{2}}^{\text{int}} < 0, \\ \frac{a_{j+\frac{1}{2}}^-}{a_{j+\frac{1}{2}}^- - u_{j+\frac{1}{2}}^{\text{int}}} & \text{otherwise,} \end{cases} \quad \delta_{j+\frac{1}{2}} = \delta_{j+\frac{1}{2}} \begin{pmatrix} 1 \\ u_{j+\frac{1}{2}}^{\text{int}} \\ \frac{1}{2} (u_{j+\frac{1}{2}}^{\text{int}})^2 \end{pmatrix}. \quad (2.12)$$

2.2.2 Semi-Discrete Scheme

We now pass to the semi-discrete limit $\Delta t^n \rightarrow 0$ in (2.11)–(2.12) and proceed as in [8, §3.1.2] to end up with the following semi-discretization

$$\frac{d}{dt} \overline{U}_j(t) = - \frac{\mathcal{F}_{j+\frac{1}{2}}(t) - \mathcal{F}_{j-\frac{1}{2}}(t)}{\Delta x}, \quad (2.13)$$

where $\mathcal{F}_{j+\frac{1}{2}}$ are the modified LDCU numerical fluxes given by

$$\mathcal{F}_{j+\frac{1}{2}} = \frac{a_{j+\frac{1}{2}}^+ \mathbf{F}(\mathbf{U}_{j+\frac{1}{2}}^-) - a_{j+\frac{1}{2}}^- \mathbf{F}(\mathbf{U}_{j+\frac{1}{2}}^+)}{a_{j+\frac{1}{2}}^+ - a_{j+\frac{1}{2}}^-} + \frac{a_{j+\frac{1}{2}}^+ a_{j+\frac{1}{2}}^-}{a_{j+\frac{1}{2}}^+ - a_{j+\frac{1}{2}}^-} (\mathbf{U}_{j+\frac{1}{2}}^+ - \mathbf{U}_{j+\frac{1}{2}}^-) + \mathbf{q}_{j+\frac{1}{2}}, \quad (2.14)$$

and

$$\mathbf{q}_{j+\frac{1}{2}} = \alpha_{j+\frac{1}{2}}^* \mathbf{q}_{j+\frac{1}{2}}^\rho \begin{pmatrix} 1 \\ u_{j+\frac{1}{2}}^* \\ \frac{1}{2} (u_{j+\frac{1}{2}}^*)^2 \end{pmatrix} \quad (2.15)$$

is a modified “built-in” anti-diffusion term with

$$\begin{aligned}
\rho_{j+\frac{1}{2}}^* &= \frac{a_{j+\frac{1}{2}}^+ \rho_{j+\frac{1}{2}}^+ - a_{j+\frac{1}{2}}^- \rho_{j+\frac{1}{2}}^- - \left[(\rho u)_{j+\frac{1}{2}}^+ - (\rho u)_{j+\frac{1}{2}}^- \right]}{a_{j+\frac{1}{2}}^+ - a_{j+\frac{1}{2}}^-}, \\
(\rho u)_{j+\frac{1}{2}}^* &= \frac{a_{j+\frac{1}{2}}^+ (\rho u)_{j+\frac{1}{2}}^+ - a_{j+\frac{1}{2}}^- (\rho u)_{j+\frac{1}{2}}^- - \left[\rho_{j+\frac{1}{2}}^+ (u_{j+\frac{1}{2}}^+)^2 + p_{j+\frac{1}{2}}^+ - \rho_{j+\frac{1}{2}}^- (u_{j+\frac{1}{2}}^-)^2 - p_{j+\frac{1}{2}}^- \right]}{a_{j+\frac{1}{2}}^+ - a_{j+\frac{1}{2}}^-}, \\
u_{j+\frac{1}{2}}^* &= \frac{(\rho u)_{j+\frac{1}{2}}^*}{\rho_{j+\frac{1}{2}}^*}, \quad \alpha_{j+\frac{1}{2}}^* = \begin{cases} \frac{a_{j+\frac{1}{2}}^+}{a_{j+\frac{1}{2}}^+ - u_{j+\frac{1}{2}}^*} & \text{if } u_{j+\frac{1}{2}}^* < 0, \\ \frac{a_{j+\frac{1}{2}}^-}{a_{j+\frac{1}{2}}^- - u_{j+\frac{1}{2}}^*} & \text{otherwise,} \end{cases} \\
q_{j+\frac{1}{2}}^\rho &= \min\text{mod}\left((u_{j+\frac{1}{2}}^* - a_{j+\frac{1}{2}}^-)(\rho_{j+\frac{1}{2}}^* - \rho_{j+\frac{1}{2}}^-), (a_{j+\frac{1}{2}}^+ - u_{j+\frac{1}{2}}^*)(\rho_{j+\frac{1}{2}}^+ - \rho_{j+\frac{1}{2}}^*)\right).
\end{aligned} \tag{2.16}$$

Note that all of the indexed quantities in (2.14)–(2.16) are time dependent, but from now on we will omit this dependence for the sake of brevity.

Remark 2.1 *As in [8], the computation of numerical fluxes in (2.14) should be desingularized to avoid division by zero or very small numbers. If $a_{j+\frac{1}{2}}^+ < \varepsilon$ and $a_{j+\frac{1}{2}}^- > -\varepsilon$ for a small positive ε , we replace the fluxes $\mathcal{F}_{j+\frac{1}{2}}$ with*

$$\mathcal{F}_{j+\frac{1}{2}} = \frac{\mathbf{F}(\mathbf{U}_{j+\frac{1}{2}}^-) + \mathbf{F}(\mathbf{U}_{j+\frac{1}{2}}^+)}{2}.$$

2.3 New LDCU Scheme for the 2-D Euler Equations of Gas Dynamics

In this section, we extend the modified semi-discrete LDCU scheme from §2.2.2 to the 2-D Euler equations of gas dynamics, which read as (1.2) with $\mathbf{U} = (\rho, \rho u, \rho v, E)^\top$, $\mathbf{F}(\mathbf{U}) = (\rho u, \rho u^2 + p, \rho uv, u(E + p))^\top$, and $\mathbf{G}(\mathbf{U}) = (\rho v, \rho uv, \rho v^2 + p, v(E + p))^\top$, where the notations are the same as in the 1-D case except for that now u and v are the x - and y -velocities, respectively. The system is closed using the EOS for the ideal gas $p = (\gamma - 1)[E - \frac{\rho}{2}(u^2 + v^2)]$.

We first introduce a uniform mesh consisting of the finite-volume cells $C_{j,k} := [x_{j-\frac{1}{2}}, x_{j+\frac{1}{2}}] \times [y_{k-\frac{1}{2}}, y_{k+\frac{1}{2}}]$ of the uniform size with $x_{j+\frac{1}{2}} - x_{j-\frac{1}{2}} \equiv \Delta x$ and $y_{k+\frac{1}{2}} - y_{k-\frac{1}{2}} \equiv \Delta y$, $j = 1, \dots, N_x$, $k = 1, \dots, N_y$. We assume that at certain time level t , an approximate solution, realized in terms of the cell averages $\bar{\mathbf{U}}_{j,k}$, is available. These cell averages are then evolved in time by solving the following system of ODEs:

$$\frac{d}{dt} \bar{\mathbf{U}}_{j,k} = -\frac{\mathcal{F}_{j+\frac{1}{2},k} - \mathcal{F}_{j-\frac{1}{2},k}}{\Delta x} - \frac{\mathcal{G}_{j,k+\frac{1}{2}} - \mathcal{G}_{j,k-\frac{1}{2}}}{\Delta y}, \tag{2.17}$$

where the x - and y -numerical fluxes are

$$\mathcal{F}_{j+\frac{1}{2},k} = \frac{a_{j+\frac{1}{2},k}^+ \mathbf{F}(\mathbf{U}_{j+\frac{1}{2},k}^-) - a_{j+\frac{1}{2},k}^- \mathbf{F}(\mathbf{U}_{j+\frac{1}{2},k}^+)}{a_{j+\frac{1}{2},k}^+ - a_{j+\frac{1}{2},k}^-} + \frac{a_{j+\frac{1}{2},k}^+ a_{j+\frac{1}{2},k}^-}{a_{j+\frac{1}{2},k}^+ - a_{j+\frac{1}{2},k}^-} (\mathbf{U}_{j+\frac{1}{2},k}^+ - \mathbf{U}_{j+\frac{1}{2},k}^-) \quad (2.18)$$

$$+ \mathbf{q}_{j+\frac{1}{2},k},$$

$$\mathcal{G}_{j,k+\frac{1}{2}} = \frac{b_{j,k+\frac{1}{2}}^+ \mathbf{G}(\mathbf{U}_{j,k+\frac{1}{2}}^-) - b_{j,k+\frac{1}{2}}^- \mathbf{G}(\mathbf{U}_{j,k+\frac{1}{2}}^+)}{b_{j,k+\frac{1}{2}}^+ - b_{j,k+\frac{1}{2}}^-} + \frac{b_{j,k+\frac{1}{2}}^+ b_{j,k+\frac{1}{2}}^-}{b_{j,k+\frac{1}{2}}^+ - b_{j,k+\frac{1}{2}}^-} (\mathbf{U}_{j,k+\frac{1}{2}}^+ - \mathbf{U}_{j,k+\frac{1}{2}}^-) \quad (2.19)$$

$$+ \mathbf{q}_{j,k+\frac{1}{2}}.$$

To obtain $\mathbf{U}_{j+\frac{1}{2},k}^\pm$ and $\mathbf{U}_{j,k+\frac{1}{2}}^\pm$ in (2.18)–(2.19), we reconstruct the second-order piecewise linear interpolant $\sum_{j,k} [\bar{\mathbf{U}}_{j,k} + (\mathbf{U}_x)_{j,k}(x - x_j) + (\mathbf{U}_y)_{j,k}(y - y_k)] \mathcal{X}_{C_{j,k}}(x, y)$ where $(\mathbf{U}_x)_{j,k}$ and $(\mathbf{U}_y)_{j,k}$ are the slopes which are supposed to be computed using a nonlinear limiter to ensure a non-oscillatory nature of the reconstruction. In the numerical experiments reported in §3, we have used the generalized minmod limiter with the minmod parameter $\theta = 1.3$. We then follow [8, §3.2] to evaluate the corresponding point values $u_{j+\frac{1}{2},k}^\pm$, $u_{j,k+\frac{1}{2}}^\pm$, $v_{j+\frac{1}{2},k}^\pm$, $v_{j,k+\frac{1}{2}}^\pm$, $p_{j+\frac{1}{2},k}^\pm$, and $p_{j,k+\frac{1}{2}}^\pm$, and estimate the one-sided local speeds of propagation $a_{j+\frac{1}{2},k}^\pm$ and $b_{j,k+\frac{1}{2}}^\pm$.

2.3.1 “Built-in” Anti-Diffusion

In this section, we discuss the derivation of the “built-in” anti-diffusion terms $\mathbf{q}_{j+\frac{1}{2},k}$ and $\mathbf{q}_{j,k+\frac{1}{2}}$ in (2.18)–(2.19) in a “dimension-by-dimension” manner following the idea introduced in [8].

In order to derive the formula for $\mathbf{q}_{j+\frac{1}{2},k}$, we consider the 1-D restriction of the 2-D system (1.2) along the lines $y = y_k$:

$$\mathbf{U}_t(x, y_k, t) + \mathbf{F}(\mathbf{U}(x, y_k, t))_x = \mathbf{0}, \quad k = 1, \dots, N_y. \quad (2.20)$$

We then go through all of the steps in the derivation of the 1-D fully discrete scheme for the systems in (2.20) following [8, §3.2] and §2 up to (2.4), which now reads as

$$\tilde{\mathbf{U}}_{j+\frac{1}{2},k}^{\text{int}}(x, y_k) = \begin{cases} \bar{\mathbf{U}}_{j+\frac{1}{2},k}^{\text{int,L}}, & x < x_{j+\frac{1}{2}} + \tilde{u}_{j+\frac{1}{2},k} \Delta t^n, \\ \bar{\mathbf{U}}_{j+\frac{1}{2},k}^{\text{int,R}}, & x > x_{j+\frac{1}{2}} + \tilde{u}_{j+\frac{1}{2},k} \Delta t^n, \end{cases}$$

and the corresponding local conservation requirements (2.5) become

$$(a_{j+\frac{1}{2},k}^+ - \tilde{u}_{j+\frac{1}{2},k}) \bar{\mathbf{U}}_{j+\frac{1}{2},k}^{\text{int,R}} + (\tilde{u}_{j+\frac{1}{2},k} - a_{j+\frac{1}{2},k}^-) \bar{\mathbf{U}}_{j+\frac{1}{2},k}^{\text{int,L}} = (a_{j+\frac{1}{2},k}^+ - a_{j+\frac{1}{2},k}^-) \bar{\mathbf{U}}_{j+\frac{1}{2},k}^{\text{int}},$$

where we take $\tilde{u}_{j+\frac{1}{2},k} = u_{j+\frac{1}{2},k}^{\text{int}} = (\overline{\rho u})_{j+\frac{1}{2},k}^{\text{int}} / \bar{\rho}_{j+\frac{1}{2},k}^{\text{int}}$. We then proceed as in [8, §3.2], where we enforce the continuity of u and p across the cell interfaces $x = x_{j+\frac{1}{2}}$ by setting

$$\frac{(\overline{\rho u})_{j+\frac{1}{2},k}^{\text{int,L}}}{\bar{\rho}_{j+\frac{1}{2},k}^{\text{int,L}}} = \frac{(\overline{\rho u})_{j+\frac{1}{2},k}^{\text{int,R}}}{\bar{\rho}_{j+\frac{1}{2},k}^{\text{int,R}}},$$

$$\bar{E}_{j+\frac{1}{2},k}^{\text{int,L}} - \frac{((\overline{\rho u})_{j+\frac{1}{2},k}^{\text{int,L}})^2 + ((\overline{\rho v})_{j+\frac{1}{2},k}^{\text{int,L}})^2}{2\bar{\rho}_{j+\frac{1}{2},k}^{\text{int,L}}} = \bar{E}_{j+\frac{1}{2},k}^{\text{int,R}} - \frac{((\overline{\rho u})_{j+\frac{1}{2},k}^{\text{int,R}})^2 + ((\overline{\rho v})_{j+\frac{1}{2},k}^{\text{int,R}})^2}{2\bar{\rho}_{j+\frac{1}{2},k}^{\text{int,R}}},$$

and enforce sharp (yet, non-oscillatory) jumps of the ρ - and ρv -components. This leads to the following formulae analogous to (2.9):

$$\begin{aligned}\bar{\rho}_{j+\frac{1}{2},k}^{\text{int,L}} &= \bar{\rho}_{j+\frac{1}{2},k}^{\text{int}} + \frac{\delta_{j+\frac{1}{2},k}^{\rho}}{a_{j+\frac{1}{2},k}^{\text{int},-}}, & \bar{\rho}_{j+\frac{1}{2},k}^{\text{int,R}} &= \bar{\rho}_{j+\frac{1}{2},k}^{\text{int}} + \frac{\delta_{j+\frac{1}{2},k}^{\rho}}{a_{j+\frac{1}{2},k}^{\text{int},+}}, \\ (\bar{\rho}v)_{j+\frac{1}{2},k}^{\text{int,L}} &= (\bar{\rho}v)_{j+\frac{1}{2},k}^{\text{int}} + \frac{\delta_{j+\frac{1}{2},k}^{\rho v}}{a_{j+\frac{1}{2},k}^{\text{int},-}}, & (\bar{\rho}v)_{j+\frac{1}{2},k}^{\text{int,R}} &= (\bar{\rho}v)_{j+\frac{1}{2},k}^{\text{int}} + \frac{\delta_{j+\frac{1}{2},k}^{\rho v}}{a_{j+\frac{1}{2},k}^{\text{int},+}},\end{aligned}$$

where $a_{j+\frac{1}{2},k}^{\text{int},\pm} := a_{j+\frac{1}{2},k}^{\pm} - u_{j+\frac{1}{2},k}^{\text{int}}$, and

$$\begin{aligned}\delta_{j+\frac{1}{2},k}^{\rho} &= \text{minmod} \left(-a_{j+\frac{1}{2},k}^{\text{int},-} [\bar{\rho}_{j+\frac{1}{2},k}^{\text{int}} - (\rho_{j+\frac{1}{2},k}^{\text{int}})_{\ell}], a_{j+\frac{1}{2},k}^{\text{int},+} [(\rho_{j+\frac{1}{2},k}^{\text{int}})_r - \bar{\rho}_{j+\frac{1}{2},k}^{\text{int}}] \right), \\ \delta_{j+\frac{1}{2},k}^{\rho v} &= \text{minmod} \left(-a_{j+\frac{1}{2},k}^{\text{int},-} [(\bar{\rho}v)_{j+\frac{1}{2},k}^{\text{int}} - ((\rho v)_{j+\frac{1}{2},k}^{\text{int}})_{\ell}], a_{j+\frac{1}{2},k}^{\text{int},+} [((\rho v)_{j+\frac{1}{2},k}^{\text{int}})_r - (\bar{\rho}v)_{j+\frac{1}{2},k}^{\text{int}}] \right),\end{aligned}$$

and the point values $(\rho_{j+\frac{1}{2},k}^{\text{int}})_{\ell}$, $(\rho_{j+\frac{1}{2},k}^{\text{int}})_r$, $((\rho v)_{j+\frac{1}{2},k}^{\text{int}})_{\ell}$, and $((\rho v)_{j+\frac{1}{2},k}^{\text{int}})_r$ were introduced in [8, Eq. (2.14)].

Next, we proceed as in §2.2 and complete the derivation of the fully discrete scheme (not shown here for the sake of brevity), and after this, we pass to the semi-discrete limit and end up with the new LDCU flux (2.18) with the following “built-in” anti-diffusion term:

$$\mathbf{q}_{j+\frac{1}{2},k} = \alpha_{j+\frac{1}{2},k}^* (q_{j+\frac{1}{2},k}^{\rho}, u_{j+\frac{1}{2},k}^*, q_{j+\frac{1}{2},k}^{\rho}, q_{j+\frac{1}{2},k}^{\rho v}, q_{j+\frac{1}{2},k}^E)^{\top}.$$

Here,

$$\begin{aligned}\mathbf{U}_{j+\frac{1}{2},k}^* &= \frac{a_{j+\frac{1}{2},k}^+ \mathbf{U}_{j+\frac{1}{2},k}^+ - a_{j+\frac{1}{2},k}^- \mathbf{U}_{j+\frac{1}{2},k}^- - [\mathbf{F}(\mathbf{U}_{j+\frac{1}{2},k}^+) - \mathbf{F}(\mathbf{U}_{j+\frac{1}{2},k}^-)]}{a_{j+\frac{1}{2},k}^+ - a_{j+\frac{1}{2},k}^-}, & u_{j+\frac{1}{2},k}^* &= \frac{(\rho u)_{j+\frac{1}{2},k}^*}{\rho_{j+\frac{1}{2},k}^*}, \\ q_{j+\frac{1}{2},k}^{\rho} &= \text{minmod} \left(-a_{j+\frac{1}{2},k}^{*, -} (\rho_{j+\frac{1}{2},k}^* - \rho_{j+\frac{1}{2},k}^-), a_{j+\frac{1}{2},k}^{*, +} (\rho_{j+\frac{1}{2},k}^+ - \rho_{j+\frac{1}{2},k}^*) \right), \\ q_{j+\frac{1}{2},k}^{\rho v} &= \text{minmod} \left(-a_{j+\frac{1}{2},k}^{*, -} ((\rho v)_{j+\frac{1}{2},k}^* - (\rho v)_{j+\frac{1}{2},k}^-), a_{j+\frac{1}{2},k}^{*, +} ((\rho v)_{j+\frac{1}{2},k}^+ - (\rho v)_{j+\frac{1}{2},k}^*) \right), \\ q_{j+\frac{1}{2},k}^E &= \frac{a_{j+\frac{1}{2},k}^{*, +} a_{j+\frac{1}{2},k}^{*, -}}{a_{j+\frac{1}{2},k}^+ - a_{j+\frac{1}{2},k}^-} \left\{ \frac{\left((\rho v)_{j+\frac{1}{2},k}^* + \frac{q_{j+\frac{1}{2},k}^{\rho v}}{a_{j+\frac{1}{2},k}^{*, +}} \right)^2}{2 \left(\rho_{j+\frac{1}{2},k}^* + \frac{q_{j+\frac{1}{2},k}^{\rho}}{a_{j+\frac{1}{2},k}^{*, +}} \right)} - \frac{\left((\rho v)_{j+\frac{1}{2},k}^* + \frac{q_{j+\frac{1}{2},k}^{\rho v}}{a_{j+\frac{1}{2},k}^{*, -}} \right)^2}{2 \left(\rho_{j+\frac{1}{2},k}^* + \frac{q_{j+\frac{1}{2},k}^{\rho}}{a_{j+\frac{1}{2},k}^{*, -}} \right)} \right\} + \frac{(u_{j+\frac{1}{2},k}^*)^2}{2} q_{j+\frac{1}{2},k}^{\rho},\end{aligned}$$

and

$$\alpha_{j+\frac{1}{2},k}^* = \begin{cases} \frac{a_{j+\frac{1}{2},k}^+}{a_{j+\frac{1}{2},k}^{*, +}} & \text{if } u_{j+\frac{1}{2},k}^* < 0, \\ \frac{a_{j+\frac{1}{2},k}^-}{a_{j+\frac{1}{2},k}^{*, -}} & \text{otherwise,} \\ \frac{a_{j+\frac{1}{2},k}^{*, -}}{a_{j+\frac{1}{2},k}^{*, +}} & \end{cases} \quad a_{j+\frac{1}{2},k}^{*, \pm} = a_{j+\frac{1}{2},k}^{\pm} - u_{j+\frac{1}{2},k}^*.$$

Similarly, the “built-in” anti-diffusion term in the new y -directional LDCU flux (2.19) is

$$\mathbf{q}_{j,k+\frac{1}{2}} = \alpha_{j,k+\frac{1}{2}}^* (q_{j,k+\frac{1}{2}}^\rho, q_{j,k+\frac{1}{2}}^{\rho u}, v_{j,k+\frac{1}{2}}^* q_{j,k+\frac{1}{2}}^\rho, q_{j,k+\frac{1}{2}}^E)^\top$$

with

$$\begin{aligned} \mathbf{U}_{j,k+\frac{1}{2}}^* &= \frac{b_{j,k+\frac{1}{2}}^+ \mathbf{U}_{j,k+\frac{1}{2}}^+ - b_{j,k+\frac{1}{2}}^- \mathbf{U}_{j,k+\frac{1}{2}}^- - [\mathbf{G}(\mathbf{U}_{j,k+\frac{1}{2}}^+) - \mathbf{G}(\mathbf{U}_{j,k+\frac{1}{2}}^-)]}{b_{j,k+\frac{1}{2}}^+ - b_{j,k+\frac{1}{2}}^-}, \quad v_{j,k+\frac{1}{2}}^* = \frac{(\rho v)_{j,k+\frac{1}{2}}^*}{\rho_{j,k+\frac{1}{2}}^*}, \\ q_{j,k+\frac{1}{2}}^\rho &= \minmod \left(-b_{j,k+\frac{1}{2}}^{*, -} (\rho_{j,k+\frac{1}{2}}^* - \rho_{j,k+\frac{1}{2}}^-), b_{j,k+\frac{1}{2}}^{*, +} (\rho_{j,k+\frac{1}{2}}^+ - \rho_{j,k+\frac{1}{2}}^*) \right), \\ q_{j,k+\frac{1}{2}}^{\rho u} &= \minmod \left(-b_{j,k+\frac{1}{2}}^{*, -} ((\rho u)_{j,k+\frac{1}{2}}^* - (\rho u)_{j,k+\frac{1}{2}}^-), b_{j,k+\frac{1}{2}}^{*, +} ((\rho u)_{j,k+\frac{1}{2}}^+ - (\rho u)_{j,k+\frac{1}{2}}^*) \right), \\ q_{j,k+\frac{1}{2}}^E &= \frac{b_{j,k+\frac{1}{2}}^{*, +} b_{j,k+\frac{1}{2}}^{*, -}}{b_{j,k+\frac{1}{2}}^+ - b_{j,k+\frac{1}{2}}^-} \left\{ \frac{\left((\rho u)_{j,k+\frac{1}{2}}^* + \frac{q_{j,k+\frac{1}{2}}^{\rho u}}{b_{j,k+\frac{1}{2}}^{*, +}} \right)^2}{2 \left(\rho_{j,k+\frac{1}{2}}^* + \frac{q_{j,k+\frac{1}{2}}^\rho}{b_{j,k+\frac{1}{2}}^{*, +}} \right)} - \frac{\left((\rho u)_{j,k+\frac{1}{2}}^* + \frac{q_{j,k+\frac{1}{2}}^{\rho u}}{b_{j,k+\frac{1}{2}}^{*, -}} \right)^2}{2 \left(\rho_{j,k+\frac{1}{2}}^* + \frac{q_{j,k+\frac{1}{2}}^\rho}{b_{j,k+\frac{1}{2}}^{*, -}} \right)} \right\} + \frac{(v_{j,k+\frac{1}{2}}^*)^2}{2} q_{j,k+\frac{1}{2}}^\rho, \end{aligned}$$

and

$$\alpha_{j,k+\frac{1}{2}}^* = \begin{cases} \frac{b_{j,k+\frac{1}{2}}^+}{b_{j,k+\frac{1}{2}}^{*, +}} & \text{if } v_{j,k+\frac{1}{2}}^* < 0, \\ \frac{b_{j,k+\frac{1}{2}}^-}{b_{j,k+\frac{1}{2}}^{*, -}} & \text{otherwise,} \end{cases} \quad b_{j,k+\frac{1}{2}}^{*, \pm} = b_{j,k+\frac{1}{2}}^\pm - v_{j,k+\frac{1}{2}}^*.$$

Remark 2.2 As in the 1-D case, the computation of numerical fluxes in (2.18) and (2.19) should be desingularized to avoid division by zero or very small numbers:

- If $a_{j+\frac{1}{2},k}^+ < \varepsilon$ and $a_{j+\frac{1}{2},k}^- > -\varepsilon$ for a small positive ε , we replace the flux $\mathcal{F}_{j+\frac{1}{2},k}$ with

$$\mathcal{F}_{j+\frac{1}{2},k} = \frac{\mathbf{F}(\mathbf{U}_{j+\frac{1}{2},k}^-) + \mathbf{F}(\mathbf{U}_{j+\frac{1}{2},k}^+)}{2};$$

- If $b_{j,k+\frac{1}{2}}^+ < \varepsilon$ and $b_{j,k+\frac{1}{2}}^- > -\varepsilon$, we replace the flux $\mathcal{G}_{j,k+\frac{1}{2}}$ with

$$\mathcal{G}_{j,k+\frac{1}{2}} = \frac{\mathbf{G}(\mathbf{U}_{j,k+\frac{1}{2}}^-) + \mathbf{G}(\mathbf{U}_{j,k+\frac{1}{2}}^+)}{2}.$$

3 Numerical Examples

In this section, we apply the developed schemes to several initial-boundary value problems for the 1-D and 2-D Euler equations of gas dynamics (with $\gamma = 1.4$) and compare the performance of the new and original second-order LDCU schemes, which will be referred to as the NEW and OLD schemes.

For time integration of the ODE systems (2.13) and (2.17), we have used the three-stage third-order strong stability preserving (SSP) Runge-Kutta method (see, e.g., [2, 3]) with the CFL number 0.475. We have taken the small desingularization parameter $\varepsilon = 10^{-12}$.

Example 1—Shock-Entropy Problem

In the first example taken from [14], we consider the shock-entropy wave interaction problem with the following initial condition:

$$(\rho(x, 0), u(x, 0), p(x, 0)) = \begin{cases} (1.51695, 0.523346, 1.805), & x < -4.5, \\ (1 + 0.1 \sin(20x), 0, 1), & x > -4.5, \end{cases}$$

which corresponds to a forward-facing shock wave of Mach number 1.1 interacting with high-frequency density perturbations, that is, as the shock wave moves, the perturbations spread ahead.

We compute the numerical solution using both the NEW and OLD schemes in the computational domain $[-5, 5]$ on a uniform mesh with $\Delta x = 1/80$. We impose the free boundary conditions by simply setting $\bar{U}_0 := \bar{U}_1$ and $\bar{U}_{N+1} := \bar{U}_N$ in the ghost cells C_0 and C_{N+1} on the left and on the right, respectively. The numerical results at time $t = 5$ are presented in Figure 3.1 along with the corresponding reference solution computed by the NEW scheme on a much finer mesh with $\Delta x = 1/800$. As one can see, the numerical solution computed by the OLD scheme is very inaccurate near the left boundary of the computational domain, while the NEW scheme accurately captures the solution throughout the entire computational domain.

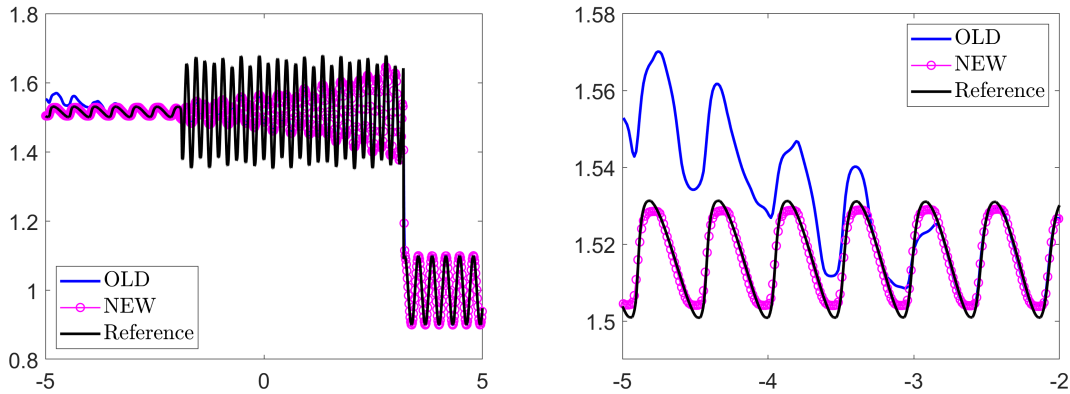


Figure 3.1: Example 1: Density ρ computed by the OLD and NEW schemes (left) and zoom at $x \in [-5, -2]$ (right).

Example 2—Stationary Contact Wave, Traveling Shock, and Rarefaction Wave

In the second example taken from [5], the initial conditions,

$$(\rho(x, 0), u(x, 0), p(x, 0)) = \begin{cases} (1, -19.59745, 1000) & \text{if } x < 0.8, \\ (1, -19.59745, 0.01) & \text{otherwise,} \end{cases}$$

are prescribed in the computational domain $[0, 1]$ subject to the free boundary conditions.

We compute the numerical solutions until the final time $t = 0.012$ using both the NEW and OLD schemes on two uniform meshes, the coarse and fine ones with $\Delta x = 1/200$ and $1/8000$, respectively. The numerical results, plotted in Figure 3.2, show that the NEW and OLD schemes achieve similar resolutions of both shock and contact waves. At the same time, the numerical results computed by the NEW scheme is non-oscillatory, while the OLD scheme solutions contain small oscillations, whose magnitude does not decay when the mesh is refined.

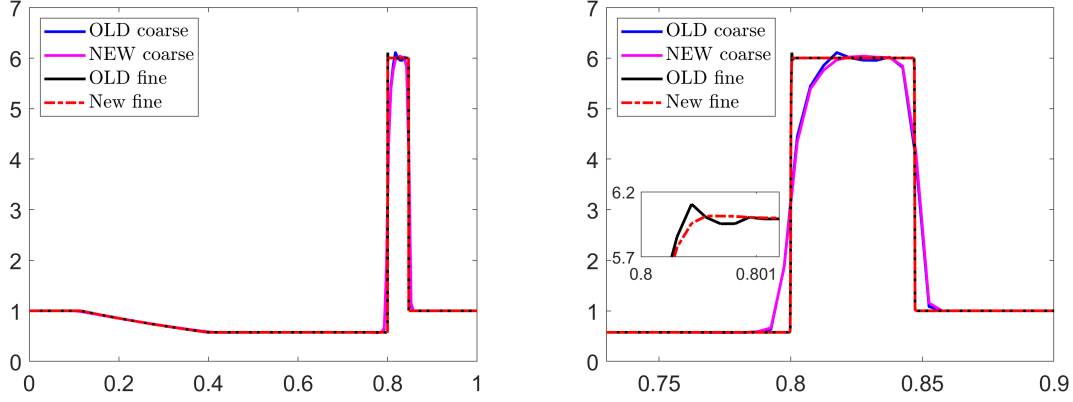


Figure 3.2: Example 2: Density ρ computed by the OLD and NEW schemes on two uniform meshes (left) and zoom at $x \in [0.7, 0.9]$ and $x \in [0.8, 0.801]$ (right).

Example 3—2-D Riemann Problem

In the first 2-D example, we consider Configuration 3 of the 2-D Riemann problems taken from [7]; see also [12, 13, 18]. The initial conditions,

$$(\rho(x, y, 0), u(x, y, 0), v(x, y, 0), p(x, y, 0)) = \begin{cases} (1.5, 0, 0, 1.5), & x > 1, y > 1, \\ (0.5323, 1.206, 0, 0.3), & x < 1, y > 1, \\ (0.138, 1.206, 1.206, 0.029), & x < 1, y < 1, \\ (0.5323, 0, 1.206, 0.3), & x > 1, y < 1, \end{cases}$$

are prescribed in the computational domain $[0, 1.2] \times [0, 1.2]$ subject to the free boundary conditions.

We compute the solution using both the NEW and OLD schemes on a uniform mesh with $\Delta x = \Delta y = 0.001$ until the final time $t = 1$ and present the obtained densities in Figure 3.3. As one can see, the NEW solution is substantially less oscillatory than the OLD one, and the resolution achieved by the NEW scheme seems to be comparable and even a little better in some parts of the computed solutions.

Example 4—Explosion Problem

In this example, we consider the explosion problem taken from [10] with the following initial conditions:

$$(\rho(x, y, 0), u(x, y, 0), v(x, y, 0), p(x, y, 0)) = \begin{cases} (1, 0, 0, 1), & x^2 + y^2 < 0.16, \\ (0.125, 0, 0, 0.1), & \text{otherwise,} \end{cases}$$

which are prescribed in the computational domain $[0, 1.5] \times [0, 1.5]$ subject to the solid wall boundary conditions at $x = 0$ and $y = 0$ and free boundary conditions at $x = 1.5$ and $y = 1.5$.

We compute the solution using the NEW and OLD schemes on a uniform mesh with $\Delta x = \Delta y = 3/800$ until the final time $t = 3.2$. The obtained densities are presented in Figure 3.4, where one can clearly see that there are obvious oscillations along the boundaries $x = 1.5$ and $y = 1.5$ in the numerical results computed by the OLD scheme, while the oscillations are substantially smaller

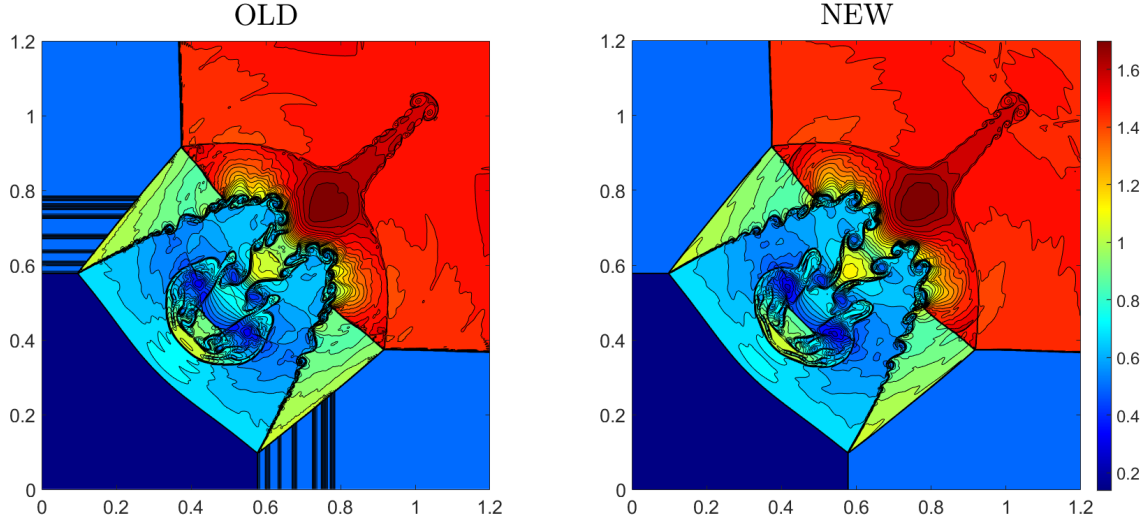


Figure 3.3: Example 3: Density (ρ) computed by the OLD (left) and NEW (right) schemes.

in the numerical results computed by the NEW scheme. At the same time, in this example, the OLD scheme achieves a slightly better resolution.

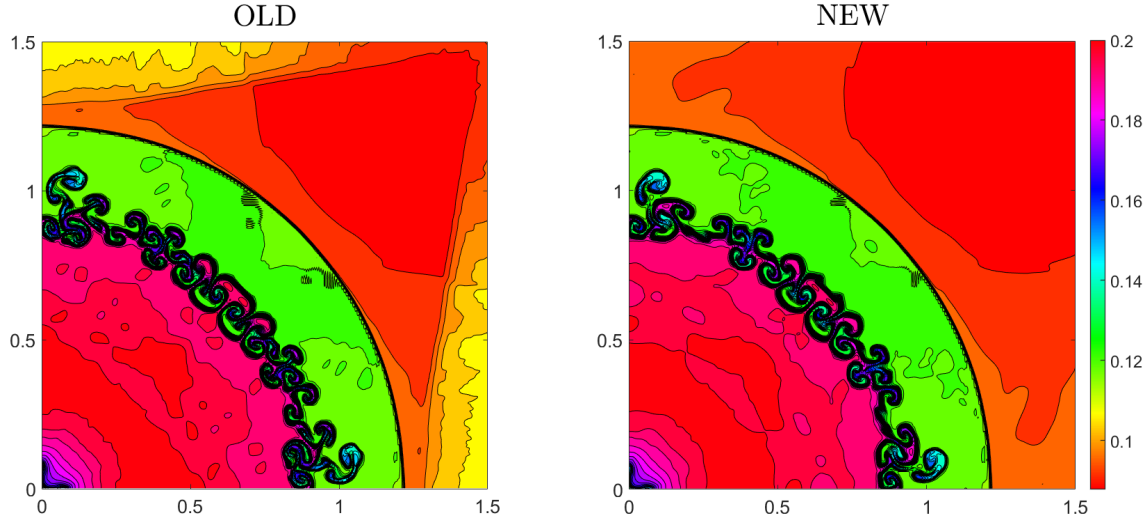


Figure 3.4: Example 4: Density (ρ) computed by the OLD (left) and NEW (right) schemes.

Example 5—Implosion Problem In the last example, we test the implosion problem also taken from [10]. The initial conditions,

$$(\rho(x, y, 0), u(x, y, 0), v(x, y, 0), p(x, y, 0)) = \begin{cases} (0.125, 0, 0, 0.14), & |x| + |y| < 0.15, \\ (1, 0, 0, 1), & \text{otherwise,} \end{cases}$$

are prescribed in the computational domain $[0, 0.3] \times [0, 0.3]$ subject to the solid wall boundary conditions.

We compute the solution using the NEW and OLD schemes on a uniform mesh with $\Delta x = \Delta y = 1/2000$ until the final time $t = 2.5$. The obtained densities are presented in Figure 3.5. As

one can see, the NEW solution is slightly less oscillatory than the OLD one. At the same time, the jet generated by the NEW scheme propagates to a larger extent than the jet produced by the OLD scheme, which demonstrates that in this example, the NEW scheme achieves slightly higher resolution than the OLD scheme.

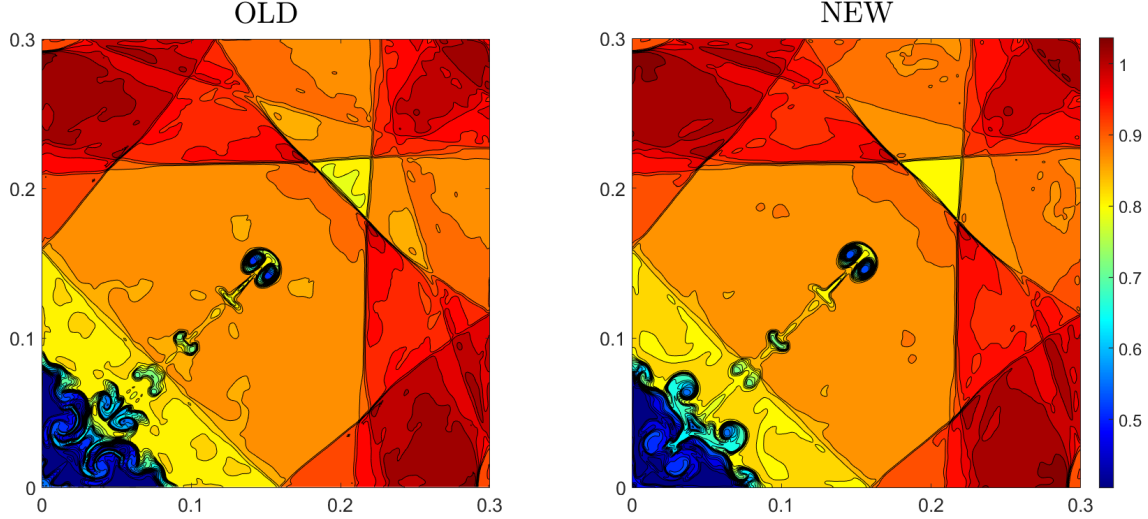


Figure 3.5: Example 5: Density (ρ) computed by the OLD (left) and NEW (right) schemes.

Declarations:

Funding. The work of A. Kurganov was supported in part by NSFC grant 12171226, and by the fund of the Guangdong Provincial Key Laboratory of Computational Science and Material Design (No. 2019B030301001).

Conflicts of interest. On behalf of all authors, the corresponding author states that there is no conflict of interest.

Data and software availability. The data that support the findings of this study and FORTRAN codes developed by the authors and used to obtain all of the presented numerical results are available from the corresponding author upon reasonable request.

References

- [1] A. CHERTOCK, S. CHU, M. HERTY, A. KURGANOV, AND M. LUKÁČOVÁ-MEDVIĐOVÁ, *Local characteristic decomposition based central-upwind scheme*, J. Comput. Phys., 473 (2023). Paper No. 111718, 24 pp.
- [2] S. GOTTLIEB, D. KETCHESON, AND C.-W. SHU, *Strong stability preserving Runge-Kutta and multistep time discretizations*, World Scientific Publishing Co. Pte. Ltd., Hackensack, NJ, 2011.

- [3] S. GOTTLIEB, C.-W. SHU, AND E. TADMOR, *Strong stability-preserving high-order time discretization methods*, SIAM Rev., 43 (2001), pp. 89–112.
- [4] A. KUGANOV, S. NOELLE, AND G. PETROVA, *Semidiscrete central-upwind schemes for hyperbolic conservation laws and Hamilton-Jacobi equations*, SIAM J. Sci. Comput., 23 (2001), pp. 707–740.
- [5] A. KURGANOV AND C.-T. LIN, *On the reduction of numerical dissipation in central-upwind schemes*, Commun. Comput. Phys., 2 (2007), pp. 141–163.
- [6] A. KURGANOV AND E. TADMOR, *New high-resolution semi-discrete central schemes for Hamilton-Jacobi equations*, J. Comput. Phys., 160 (2000), pp. 720–742.
- [7] A. KURGANOV AND E. TADMOR, *Solution of two-dimensional Riemann problems for gas dynamics without Riemann problem solvers*, Numer. Methods Partial Differential Equations, 18 (2002), pp. 584–608.
- [8] A. KURGANOV AND R. XIN, *New low-dissipation central-upwind scheme*, J. Sci. Comput., 96 (2023). Paper No. 56, 33 pp.
- [9] K.-A. LIE AND S. NOELLE, *On the artificial compression method for second-order nonoscillatory central difference schemes for systems of conservation laws*, SIAM J. Sci. Comput., 24 (2003), pp. 1157–1174.
- [10] R. LISKA AND B. WENDROFF, *Comparison of several difference schemes on 1D and 2D test problems for the Euler equations*, SIAM J. Sci. Comput., 25 (2003), pp. 995–1017.
- [11] H. NESSYAHU AND E. TADMOR, *Nonoscillatory central differencing for hyperbolic conservation laws*, J. Comput. Phys., 87 (1990), pp. 408–463.
- [12] C. W. SCHULZ-RINNE, *Classification of the Riemann problem for two-dimensional gas dynamics*, SIAM J. Math. Anal., 24 (1993), pp. 76–88.
- [13] C. W. SCHULZ-RINNE, J. P. COLLINS, AND H. M. GLAZ, *Numerical solution of the Riemann problem for two-dimensional gas dynamics*, SIAM J. Sci. Comput., 14 (1993), pp. 1394–1414.
- [14] C.-W. SHU AND S. OSHER, *Efficient implementation of essentially non-oscillatory shock-capturing schemes*, J. Comput. Phys., 77 (1988), pp. 439–471.
- [15] P. K. SWEBY, *High resolution schemes using flux limiters for hyperbolic conservation laws*, SIAM J. Numer. Anal., 21 (1984), pp. 995–1011.
- [16] B. VAN LEER, *Towards the ultimate conservative difference scheme. V. A second-order sequel to Godunov’s method*, J. Comput. Phys., 32 (1979), pp. 101–136.
- [17] P. WOODWARD AND P. COLELLA, *The numerical solution of two-dimensional fluid flow with strong shocks*, J. Comput. Phys., 54 (1988), pp. 115–173.
- [18] Y. ZHENG, *Systems of conservation laws: Two-dimensional Riemann problems*, Progress in Nonlinear Differential Equations and their Applications, 38, Birkhäuser Boston, Inc., Boston, MA, 2001.